Opposing Effects of Bacitracin on Human Papillomavirus Type 16 Infection: Enhancement of Binding and Entry and Inhibition of Endosomal Penetration

Samuel K. Campos,[a,b] **Janice A. Chapman,**[b] **Martin J. Deymier,**[c*] **Matthew P. Bronnimann,**[d] **and Michelle A. Ozbun**[e]

Department of Immunobiology,[a] BIO5 Institute,[b] Department of Molecular and Cellular Biology,[c] and Department of Veterinary Science and Microbiology,[d] The University of Arizona, Tucson, Arizona, USA, and Department of Molecular Genetics and Microbiology, The University of New Mexico, Albuquerque, New Mexico, USA[e]

Cell invasion by human papillomavirus type 16 (HPV16) is a complex process relying on multiple host cell factors. Here we describe an investigation into the role of cellular protein disulfide isomerases (PDIs) by studying the effects of the commonly used PDI inhibitor bacitracin on HPV16 infection. Bacitracin caused an unusual time-dependent opposing effect on viral infection. Enhanced cellular binding and entry were observed at early times of infection, while inhibition was observed at later times postentry. Bacitracin was rapidly taken up by host cells and colocalized with HPV16 at late times of infection. Bacitracin had no deleterious effect on HPV16 entry, capsid disassembly, exposure of L1/L2 epitopes, or lysosomal trafficking but caused a stark inhibition of L2/viral DNA (vDNA) endosomal penetration and accumulation at nuclear PML bodies. γ-Secretase has recently been implicated in the endosomal penetration of L2/vDNA, but bacitracin had no effect on γ-secretase activity, indicating that blockage of this step occurs through a γ-secretase-independent mechanism. Transient treatment with the reductant β-mercaptoethanol (β-ME) was able to partially rescue the virus from bacitracin, suggesting the involvement of a cellular reductase activity in HPV16 infection. Small interfering RNA (siRNA) knockdown of cellular PDI and the related PDI family members ERp57 and ERp72 reveals a potential role for PDI and ERp72 in HPV infection.

Human papillomaviruses (HPVs) are one of the most common sexually transmitted infections in the world. HPVs are small 55-nm icosahedral nonenveloped double-stranded DNA (dsDNA) viruses that replicate in differentiating cutaneous and mucosal epithelium. Infection of mucosal epithelium by oncogenic HPV genotypes can lead to cervical, anogenital, and other head and neck cancers. HPV type 16 (HPV16) is the most common of the high-risk types and is alone responsible for over 50% of cervical cancers worldwide (77). Although HPVs have been known to be the etiological agent of cervical cancer for nearly 30 years, and despite intensive research in recent years, the infectious entry pathway of HPV16 is still not well defined. Our current understanding of HPV cellular invasion reveals a complex and prolonged process, complicated by differences between *in vitro* cell culture systems and the recently described *in vivo* mouse cervicovaginal challenge model (33, 37, 50, 62).

The HPV capsid is assembled from 360 molecules of the L1 protein, arranged as 72 pentamers. L1 monomers from neighboring pentamers are disulfide bonded to each other as dimers and trimers, providing stability to the capsid (45). The minor capsid protein L2 is localized within a central cavity beneath the L1 pentamers. L2 can be present at a maximum stoichiometry of one L2 molecule per L1 pentamer or 72 molecules per virion; however, most preparations of virus contain submaximal levels of L2, typically 20 to 25 copies per virion (6). Packaged within the capsid is the ~8-kb viral genome (viral DNA [vDNA]), condensed as chromatin with cellular histones and complexed with L2.

In vitro HPV16 attachment to host cell membranes occurs through heparan sulfate proteoglycans (HSPGs). HPV16 can also bind to secreted extracellular matrix (ECM) via laminin 5 and/or HSPGs, and ECM-bound virus is believed to have the capacity to transfer to the cell membrane (55, 69). *In vivo*, HPV16 initially binds to HSPGs on the basement membrane (BM) before transfer

to a non-HSPG cell surface receptor on basal keratinocytes (33, 37, 62). During a prolonged residence time on the cell surface (*in vitro*) or BM (*in vivo*), the virus undergoes a series of conformational changes, losing affinity for HSPGs and exposing concealed regions of L1 and L2 which facilitate transfer to a non-HSPG entry receptor and expose the furin cleavage site ⁹RTKR¹² near the N terminus of L2 (15, 55, 62, 64). There is evidence that cell surface cyclophilin B (CyPB) is involved in isomerization of a specific proline residue in L2 to promote exposure of the furin cleavage site (4). Cleavage of L2 by furin on the cell surface or the BM then triggers exposure of another N-terminal portion of L2, residues 17 to 36 (13). This region of L2 is a B-cell epitope, and the RG-1 monoclonal antibody against this epitope will neutralize HPV16 infection (22). Exposure of the RG-1 epitope is not needed for viral entry but is essential at the later stage of endosomal penetration, as furin inhibitors which block RG-1 epitope exposure prevent endosomal escape of the L2/vDNA complex (49).

Our current understanding of the HPV entry pathway is incomplete and under debate. The most recent work suggests that HPV16 internalization can occur through novel clathrin-, caveolin-, lipid raft-, and dynamin-independent entry routes that involve the phosphatidylinositol 3-kinase (PI3 kinase) signaling

pathway, growth factor receptor signaling, and actin remodeling (56, 60, 70, 72). Internalized HPV16 is sorted into the endosomal system, where low pH is believed to trigger disassembly of the capsid, enabling endosomal penetration by L2 and cytosolic translocation of the L2/vDNA complex (34, 68). A recent study showed that cellular γ-secretase, a membrane aspartyl protease complex that cleaves transmembrane (TM) domains, is essential for L2-dependent endosomal membrane penetration, although the mechanisms are unknown (36). Once in the cytoplasm, the L2/vDNA likely associates with components of the dynein microtubule motor for transport toward the nucleus (19, 63). Cellular Hsc70 may be involved in transfer of L2 from dynein to the nucleus (20), although the exact nature of L2/vDNA nuclear import is not known. Once in the nucleus, L2 localizes the vDNA to PML bodies, a key step for transcription of early genes and establishment of infection (12).

An emerging theme in our understanding of HPV16 infection is the dependence on a number of cellular enzymatic factors (furin, CyPB, and γ-secretase) for facilitating the changes in capsid conformation that underlie the critical steps of infection. The oxidized nature of the HPV virion and the highly conserved cysteine residues and disulfide bonds in both the L1 and L2 capsid proteins (7, 8, 30, 38, 45, 57) as well as the involvement of protein disulfide isomerases (PDIs) and disulfide redox chemistry in the structurally related polyomaviruses (23, 40, 61, 78) prompted us to investigate whether PDIs play a similar role in HPV16 infection. The PDI family consists of ~20 enzymes that catalyze the oxidation, reduction, and isomerization or shuffling of disulfide bonds in protein substrates, thereby playing a crucial role in folding and refolding of nascent and misfolded proteins in the endoplasmic reticulum (ER) (17). Although the PDI family members are primarily localized to the ER, there is growing evidence for non-ER locations and functions (32, 75). Since the PDI family encompasses nearly 20 distinct proteins, an inhibitor-based approach was used to investigate the role(s) of PDIs in HPV16 infection.

Commonly used PDI inhibitors include thiol-reactive compounds like 5,5′-dithiobis-2-nitrobenzoic acid (DTNB) and p-chloromercuribenzenesulfonic acid (pCMBS), which inactivate PDIs by covalently bonding with the reactive cysteine thiolate of the PDI active site. We and others have observed that thiol-reactive compounds block HPV16 infection through direct modification of L1 cysteine residues on the capsid (S. Campos et al., unpublished data; also see reference 29), preventing the use of these reagents for studies on PDIs. We therefore chose to use another frequently used inhibitor of PDI activity, the cyclic peptide antibiotic bacitracin (Bac). Here we show that Bac causes unusual time-dependent effects on HPV16 infectivity, enhancing cellular binding and entry at early times of infection and blocking endosomal penetration of the vDNA at late times postentry. Bac had no inhibitory effects on viral entry, uncoating, lysosomal trafficking, or capsid conformational changes and exposure of hidden L1 and L2 epitopes. Bac itself was rapidly taken up by cells and colocalized with virus at late times postinfection. Infection could be partially rescued from the inhibitory effects of Bac by a reducing agent, suggesting that a cellular reductive function may be important for endosomal penetration of L2/vDNA and HPV16 infection. Small interfering RNA (siRNA) knockdown experiments implicate PDI and ERp72 in HPV16 infection and as potential cellular targets for bacitracin.

MATERIALS AND METHODS

Preparation of bacitracin. Bac (Sigma B0125) was dissolved to 20 mM in complete medium, and phenylmethylsulfonyl fluoride (PMSF) (Sigma P7626) was added to a 1 mM final concentration. The solution was incubated for at least 6 h at room temperature in the dark to allow for the irreversible inactivation of protease activity by PMSF. PMSF is unstable in aqueous solution, and any unreacted PMSF will hydrolyze during this prolonged incubation. Bac solution was then filtered through a 0.2-μm filter, aliquoted, and stored at −20°C.

Cells and viruses. 293TT, HeLa, MRC5, and U373 cells were cultured in Dulbecco's modified Eagle medium (DMEM) high-glucose medium (Sigma D5796) supplemented with 10% bovine growth serum (BGS) (HyClone SH30541.03) and antibiotic/antimycotic (Sigma A5955). 293TT cells were maintained with 0.4 μg/ml hygromycin B (Roche 30-240-CR). HaCaT, ARPE-19, and murine 308 cells were cultured in DMEM–Ham's F-12 medium (Sigma D6421), supplemented with 10% BGS, 4× minimal essential medium (MEM) amino acids (Sigma M5550), and L-glutamine–penicillin–streptomycin (Sigma G1146). For infections, HaCaT cells were cultured in medium containing fetal bovine serum (FBS) (HyClone SH30396.03) rather than BGS. Virions containing luciferase- (pGL3-basic) or green fluorescent protein (GFP)-expressing (pCIneoGFP) reporter plasmids or recircularized HPV16 genome were produced by CaPO$_4$ transfection of 293TT cells and purified by CsCl density gradient centrifugation as previously described (8, 48, 67). Purified virions were assayed for purity and L1 protein content against bovine serum albumin (BSA) standards by SDS-PAGE and Coomassie blue staining and for genome content by SYBR green quantitative PCR (qPCR). Turbofect reagent (Fermentas R0531) was used for transfections. The λ-secretase inhibitor XXI, (S-S)-2-[2-(3,5-difluorophenyl)-acetylamino]-N-(1-methyl-2-oxo-5-phenyl-2,3-dihydro-1H-benzo[e][1,4]diazepin-3-yl)-propionamide (catalog no. 565790; EMD Biosciences), was used at a concentration of 1 μM, and DAPT, N-[3,5-difluorophenyl)acetyl]-L-alanyl-2-phenyl]glycine-1,1-dimethylethyl ester (catalog no. 2634; Tocris Bioscience), was used at a concentration of 10 μM.

Infections. HaCaT cells were plated in 24-well plates and infected in 0.5 to 1 ml medium at a multiplicity of infection (MOI) of 1,000 to 2,000 viral genomes per cell. Viral inoculum was left on cells for 24 h or indicated times for continuous infections, or synchronized infections were set up by binding virus to cells at 4°C for 1 h followed by washing of excess unbound virus and transfer of cells to 37°C to initiate infection. At 48 h, cells were lysed in 0.1 ml 1× reporter lysis buffer (RLB) (Promega E3971) and infection was measured with a DTX-800 multimode plate reader (Beckman Coulter) by firefly luciferase assay according to the manufacturer's recommendations (Promega E4550). For some experiments, lysates were normalized to protein content by the Bradford assay (Pierce 23236). For imaging experiments, HaCaT cells were plated on glass coverslips and infected with HPV16 at 0.25 to 0.5 μg virus in 1 ml medium with or without drugs for various lengths of time prior to further processing.

siRNA knockdown experiments. Pools of three siRNA duplexes against PDI (sc36201), ERp57 (sc35341), and ERp72 (sc44571) and a scramble control (sc37007) were obtained from Santa Cruz. HaCaT cells were transfected with 50 nM siRNAs using Lipofectamine RNAiMax reagent (Invitrogen 13778-075) in 24-well plates. At 24 h after siRNA transfection, cells (now ~60% confluent) were rinsed with phosphate-buffered saline (PBS) and infected with HPV16. Infection was quantified 24 h posttransfection, and infection lysates were analyzed for protein knockdown by Western blotting. Four independent experiments were performed, each in triplicate.

Nonreducing gels and Western blots. Samples were diluted into nonreducing SDS-PAGE loading buffer (62.5 mM Tris, pH 6.8, 10% glycerol, 2% SDS, 0.5% bromophenol blue, 4 mM N-ethylmaleimide) and incubated for 10 min at room temperature to inactivate free thiols prior to passage through a Qiashredder column and loading on a 10% Tris-glycine

polyacrylamide gel. Gels were transferred to a polyvinylidene difluoride (PVDF) membrane and blocked in Tris-buffered saline–Tween (TBST) plus 4% milk, 4% BSA, and 1% goat serum. Mouse anti-L1 (Abcam ab30908), mouse anti-Myc (Genscript A00704), and mouse antitubulin (Cell Signaling 3873) were all used at 1:5,000 in TBST plus 20% block. Mouse anti-PDI (Abcam ab2792, clone RL90) was used at 1:5,000, rabbit anti-ERp72 (Cell Signaling 2798) and rabbit anti-ERp57 (Cell Signaling 2881) were used at 1:300, and rabbit anti-glyceraldehyde-3-phosphate dehydrogenase (anti-GAPDH) (Cell Signaling 2118) was used at 1:3,000 in TBST plus 20% block. Goat anti-mouse and anti-rabbit horseradish peroxidase (HRP)-labeled secondary antibodies (Abcam ab6789 and ab6721, respectively) were used at 1:10,000 in TBST plus 20% block. Supersignal West Pico chemiluminescent substrate (Pierce 34080) was used. Films were scanned, and images were processed with Adobe Photoshop software.

EdU labeling and detection. HPV virions containing 5-ethynyl-2′-deoxyuridine (EdU)-labeled pGL3-basic DNA were produced by transfection of 293TT cells. The Click-iT EdU imaging kit (Invitrogen C10337) was used for EdU labeling and detection. Briefly, 293TT cells were maintained in complete DMEM (cDMEM) supplemented with 15 μM EdU before and during the CaPO$_4$ transfection. EdU-labeled virions were used to track viral genome (vDNA) during infection of HaCaT cells and assay for colocalization with nuclear PML bodies at late times postinfection. Cells were seeded on glass coverslips and infected with EdU-labeled HPV at 500 ng/ml with or without 5 mM Bac or 16 nM bafilomycin A (BafA) for 18 h. Medium was then replaced with or without drugs, and cells were cultured for an additional 24 h. At 42 h postinfection, cells were chilled to 4°C, washed 3 times in cold PBS, and fixed with acetone at −20°C for 5 min. Cells were blocked at 4°C overnight in PBS plus 4% BSA and 1% goat serum, and EdU-labeled vDNA was conjugated to Alexa Fluor 488-N$_3$ by CuSO$_4$-catalyzed click chemistry (54), according to the manufacturer's instructions (Invitrogen C10337). Cells were then washed and immunostained with rabbit anti-PML polyclonal antibody (Abcam ab53773) at 1:300 and the L1-7 mouse anti-L1 monoclonal antibody (kind gift of Martin Sapp) at 1:100. Alexa Fluor 555 goat anti-rabbit and Alexa Fluor 633 goat anti-mouse (Molecular Probes A21052) were used at 1:1,000 dilutions. After staining, coverslips were mounted on slides in Prolong Gold Antifade medium containing 4′,6-diamidino-2-phenylindole (DAPI) (Molecular Probes P36931).

Immunofluorescence (IF). With the exception of the EdU-labeled samples, cellular specimens were fixed with PBS plus 2% paraformaldehyde for 10 min at room temperature, permeabilized with PBS plus 0.2% Triton X-100 for 5 min at room temperature, and blocked in PBS plus 4% BSA and 1% goat serum prior to immunostaining. The rabbit anti-L1 polyclonal antibody K75 and mouse anti-L1 monoclonal antibody L1-7 (kind gifts of Martin Sapp) were used at 1:5,000 and 1:100, respectively. Sheep antibacitracin (Abnova PAB8227) was used at 1:500. Rabbit anti-EEA1 (Cell Signaling 3288), rabbit anti-Rab7 (Cell Signaling 2094), rabbit anticalnexin (Cell Signaling 2433), rabbit anti-flotillin 2 (Cell Signaling 3436), rabbit anti-caveolin 1 (Cell Signaling 3267), rabbit anti-syntaxin 6 (Cell Signaling 2869), rabbit anti-PDI (Abcam ab3672), mouse anti-clathrin light chain (Abcam 24579), mouse anti-LAMP1 (Abcam 25630), mouse antigiantin (Abcam 37266), and mouse anti-CD44 (Cell Signaling 5640) were all used at a 1:250 dilution. Rabbit anti-ERp72 (Cell Signaling 5033) was used at 1:100. H16.U4 mouse anti-L1 monoclonal antibody (a kind gift from Neil Christensen) was used at a 1:200 dilution. The RG-1 anti-L2 monoclonal antibody (a kind gift from Richard Roden) was used at a 1:200 dilution, and immunostaining of live cells prior to fixation was performed as described in reference 13. Alexa Fluor-labeled goat anti-mouse and anti-rabbit secondary antibodies (Molecular Probes) were used at 1:1,000. To avoid potential cross-reactivity between goat and sheep species, goat serum was omitted from the block and donkey secondary antibodies were used in conjunction with sheep antibacitracin and AF555 donkey anti-sheep antibody.
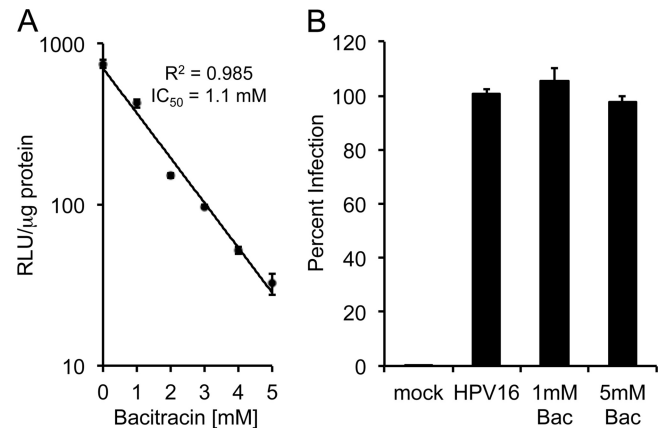

FIG 1 Bacitracin blocks HPV16 infection via a cellular process. (A) Continuous infection of HaCaT cells in the presence of increasing concentrations of Bac. Infection was quantified after 48 h by luciferase assay. RLU, relative light units. (B) Virus was pretreated with 1 mM or 5 mM Bac in cell culture medium for 8 h at 37°C. Virus was then diluted into complete medium such that the final Bac concentration was well below the inhibitory concentrations, and infection was assayed by luciferase assay. Infections were performed in triplicate, with error bars representing standard errors of the means.

Confocal microscopy. Specimens were examined on a Zeiss Axiovert 200 inverted microscope with a 63× objective. Confocal microscopy was performed with the Zeiss LSM 510 Meta system using the 405-nm laser diode, 488-nm argon laser, 543-nm He/Ne1 laser, and 633-nm He/Ne2 laser excitations. Z stacks of several (4 to 9 slices) 1-μm-thick optical slices were scanned in 0.2-μm increments for colocalization analysis. Select images were processed with Adobe Photoshop and Microsoft Powerpoint software.

Colocalization analysis. The JACoP plugin (5) for the ImageJ software package (1) was used to quantify the Manders coefficient of colocalization for the Z stacks. Thresholds were manually set, and colocalization analysis was performed on three separate Z stacks, each containing 4 to 7 slices. Results are presented as an average colocalization ± standard deviation. Using the Manders coefficient in this way provides a readout for percent Bac overlap with the cellular marker signal in Fig. 3B and percent HPV16 L1 overlap with Bac signal in Fig. 3C.

RESULTS

Bacitracin inhibition of HPV infection. Commercial Bac contains a protease contaminant (51) and was prepared with complete medium containing 10% serum and PMSF as described in Materials and Methods to eliminate the contaminant protease activity (see Fig. S1B in the supplemental material). HaCaT cells were infected with luciferase-expressing HPV16 virions in the presence of increasing concentrations of Bac for 48 h. Quantification of infection revealed a dose-dependent inhibition of HPV16 infection, with a 50% inhibitory concentration (IC$_{50}$) of 1.1 mM (Fig. 1A). A 90 to 95% inhibition was routinely measured in the presence of 5 mM Bac. The millimolar concentrations of Bac required for inhibition are within range of the reported concentrations for PDI inhibition (26, 41, 53, 66). Control medium prepared with PMSF but lacking Bac showed no inhibition of infection, ruling out any effect from the PMSF hydrolysis products. (see Fig. S1C). Similar inhibition of HPV16 was observed using virions packaged with a GFP reporter plasmid or with circular HPV16 viral genome (see Fig. S2A and B), ruling out a luciferase-specific effect. Unlike thiol-reactive PDI inhibitors, pretreatment of purified HPV16 with Bac for 8 h at 37°C had no effect
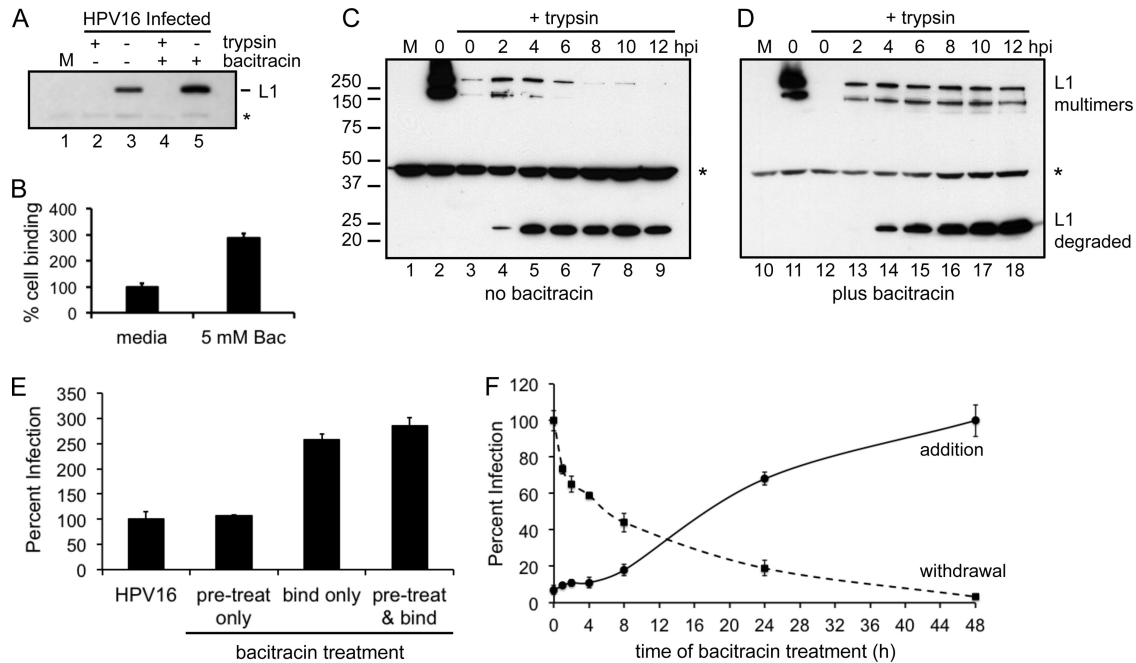
FIG 2 Time-dependent effects of bacitracin. (A) Binding assay. Virus was bound to cells in medium with or without 5 mM Bac for 1 h at 4°C. Cells were then thoroughly washed and either trypsin or mock treated before harvesting of total protein by the addition of SDS-PAGE loading buffer. Cell-associated L1 was detected by Western blotting with an anti-L1 monoclonal antibody. The asterisk denotes a nonspecific band of cellular origin. (B) Quantification of the band intensities from three separate binding assays. (C and D) Virus uptake assay in the absence (C) or presence (D) of 5 mM Bac. Cells were mock infected (M, lanes 1 and 10) or prebound with virus and either processed immediately (0 h, lanes 2 and 11, the bound input virus) or trypsinized after various lengths of time at 37°C (lanes 3 to 9 and 12 to 18) before processing for nonreducing SDS-PAGE and Western blotting for L1. Molecular masses (kDa) are shown to the left, and positions of the L1 forms are denoted on the right. The asterisk again denotes the nonspecific band. (E) Bac-induced binding and entry occur through the infectious pathway. Infections were set up with or without Bac pretreatment and with or without Bac during virus binding as described in the text. Cells were washed and switched to 37°C, and infection was measured at 48 h by luciferase assay. (F) Time of addition/withdrawal experiments. Cells were bound with virus in medium with or without Bac and washed, and medium with or without Bac was replaced. After various times at 37°C, medium was changed to add Bac (time of addition, solid line) or to remove Bac (time of withdrawal, dashed line). The highest levels of infection for each experiment were normalized to 100%. All infections were performed in triplicate, with error bars representing standard errors of the means.

on infectivity (Fig. 1B), implying that the Bac-dependent blockage was caused by inhibition of some cellular process rather than a direct effect on the virus. Bac had negligible cellular toxicity at the concentrations used, and Bac did not inhibit infection by adenoviral vectors (see Fig. S2C and D), suggesting that HPV16 inhibition was not due to some overt cell toxicity or general inhibition of critical processes like endocytosis, gene expression, or protein synthesis. Bac caused similar inhibition of a broad range of HPV types, including high-risk HPV31, HPV58, HPV18, and HPV45; low-risk HPV6; and cutaneous types HPV2 and HPV5, although HPV18 and HPV45 appeared to be less sensitive to the drug (see Fig. S3A). Bac inhibition was not limited to HaCaT keratinocytes, as it also blocked HPV16 infection of HeLa cervical carcinoma cells, ARPE-19 retinal pigment epithelial cells, MRC5 lung fibroblast cells, U373 astrocytoma cells, and murine 308 keratinocytes (see Fig. S3B).

Bacitracin enhances HPV16 cell binding and uptake. The mechanisms of Bac-mediated HPV16 inhibition were first investigated by a cell binding assay. Subconfluent HaCaT cells were mock treated or exposed to HPV16 with or without Bac for 1 h at 4°C, and unbound virus was washed away. An aliquot of cells was trypsinized to remove bound virus prior to assay for L1 protein by SDS-PAGE and Western blotting. Surprisingly, Bac caused an increase in cell binding (Fig. 2A, compare lanes 3 to 5). All samples treated with trypsin prior to SDS-PAGE were devoid of L1 signal

(Fig. 2A, lanes 2 and 4), indicating that these viruses were surface bound. Quantification of the binding results by densitometry shows nearly a 3-fold increase in virus binding with 5 mM Bac (Fig. 2B).

Next, the effects of Bac on HPV16 cell entry and capsid disassembly were investigated by nonreducing SDS-PAGE and Western blotting. HaCaT cells were mock treated or exposed to HPV16 with or without Bac at 4°C as before. Cells were then washed and either immediately processed for SDS-PAGE and measurement of bound virus or switched to medium at 37°C for different times prior to trypsinization (to remove surface virus) and detection of internalized virus by SDS-PAGE and Western blotting for L1. Nonreducing SDS-PAGE conditions were used to keep L1s in their native disulfide-bonded state (dimers and trimers) and monitor reduction of L1 to a monomeric ~52-kDa form during entry and intracellular trafficking as shown for the structurally related polyomavirus simian virus 40 (SV40) (61). During normal infection, a spike in the intracellular levels of multimeric L1 was observed 2 to 4 h postinfection (Fig. 2C, lanes 4 and 5), with these levels decreasing over time and essentially disappearing by the latter times (Fig. 2C, lanes 7 to 9), indicative of a wave of incoming viral particles entering the cell within the first 2 to 4 h. Concomitant with the disappearance of the multimeric L1 was the appearance of a 25-kDa species, most likely a proteolytic degradation product. Levels of this 25-kDa form peaked by 4 h and remained

steady throughout the infection time course (Fig. 2C, lanes 5 to 9). At no time during infection was there an appearance of the 52-kDa monomeric (reduced) form of L1, suggesting that capsid disassembly involves proteolytic degradation rather than reduction of the disulfide-linked L1 multimers.

Bac caused a striking difference in the dynamics of HPV16 uptake. The increased cell binding was again evident as the blot exposure time in Fig. 2D was shorter than that of Fig. 2C, as can be seen by the relative signals for the nonspecific cellular protein band at ~47 kDa (marked with an asterisk). Intracellular levels of disulfide-linked multimeric L1 stayed relatively constant during the time course while levels of the 25-kDa degradation product increased steadily in the presence of Bac (Fig. 2D, lanes 13 to 18). These dynamics support a steady-state mode of continual entry in response to Bac, unlike the more synchronized wave of viral uptake observed under normal conditions.

Bacitracin mediates enhanced binding and uptake through the infectious pathway. The observed increase of HPV16 binding and entry in response to Bac is inconsistent with its inhibitory effects on infection. One explanation is that Bac may redirect viral binding and entry through a nonproductive pathway. Soluble heparin neutralizes HPV16 infection of HaCaT cells by specifically blocking cell membrane binding, resulting in the sequestration of virions to the underlying ECM (16). In contrast, neutralization by the HPV16-specific monoclonal antibody H16.V5 (10) enables HSPG binding but blocks ECM binding and prevents viral uptake by inhibiting transfer from HSPGs to the entry receptor (16). To determine if HPV16 virus-cell interactions were proceeding through the infectious pathway in the presence of Bac, we first investigated the mechanisms of heparin and H16.V5 neutralization of Bac-mediated binding and entry. Bac caused no change in the heparin or H16.V5 neutralization pattern of HPV16 infection (see Fig. S4 in the supplemental material).

These neutralization data suggest that enhanced entry in the presence of Bac happens via the infectious pathway used by HPV16. Additional infection experiments were designed to directly test if Bac-induced binding truly led to enhanced infection. Subconfluent HaCaT cells were pretreated with medium with or without 5 mM Bac for 1 h at 4°C. Cells were then washed with cold medium, and HPV16 was bound to both groups of cells in cold medium with or without Bac for an additional 1 h at 4°C. Cells were washed again and incubated in fresh medium for 48 h prior to measurement of infection by luciferase assay. Bac pretreatment of cells at 4°C caused no change in HPV16 infectivity (Fig. 2E). Regardless of the pretreatment condition, the addition of Bac during the binding step resulted in enhanced levels of infection (Fig. 2E). The nearly 3-fold increase in HPV16 infection correlated well with the enhanced binding observed in Fig. 2A and B, and together these data confirm that the enhanced binding and entry do indeed occur through the infectious pathway.

Bacitracin inhibition occurs at a late stage postentry. To better understand the mechanisms of Bac inhibition, we performed infection experiments varying the times of Bac addition or withdrawal. Experiments where 5 mM Bac was present throughout the 48-h infection resulted in 90 to 95% inhibition. In the Bac addition experiments, HPV16 was bound to HaCaT cells in cold medium, washed, and switched to 37°C to allow infection for various amounts of time before the addition of Bac for the 48-h duration of infection. Addition of Bac at 0 to 4 h postinfection caused ≥90% inhibition and caused an 80 to 85% inhibition when added

as late as 8 h postinfection, suggesting a block during the latter stages of cell infection. Addition of Bac after 24 h caused ~30% inhibition (Fig. 2F, solid line).

Bac withdrawal experiments were set up in a similar manner, with Bac present during the cold binding step and in the growth medium during infection at 37°C. After various lengths of time, Bac-containing media were switched to normal media and cells were returned to 37°C for the duration of infection. Removal of Bac immediately after the binding step (time zero) resulted in the highest levels of infection. Just 30 min of Bac treatment during infection at 37°C, before drug removal, resulted in a 20 to 25% decrease in infection levels (Fig. 2F, dashed line). This trend continued with 4-h and 8-h Bac treatments resulting in 40% and 55% inhibition, respectively, and 24 h of Bac exposure resulting in ~80% inhibition of HPV16 infection (Fig. 2F, dashed line). Interpretation of the withdrawal experiments is confounded by the enhanced and continual entry effect caused by Bac during the initial binding stages (Fig. 2A, B, and D). In addition, the unknown cellular pharmacodynamics between Bac and HaCaT cells may further complicate interpretation of the time-dependent Bac inhibition profiles.

Bacitracin is endocytosed in HaCaT cells and colocalizes with HPV16 during infection. Bac is a relatively large compound with several charged groups (see Fig. S1A in the supplemental material). The molecule is membrane impermeant (data not shown) and has been widely cited for use as a "cell surface" PDI inhibitor due to its inability to cross the cell membrane (2, 41, 53). Our data support impairment of HPV16 at a late stage (>8 h) postinfection, well after the bulk of viral entry (Fig. 2F). These observations are inconsistent with the cell-impermeant nature of Bac, and we hypothesized that the drug may enter cells through endocytic uptake. Cells were grown in 5 mM Bac for 1 h at 37°C and either processed immediately for immunofluorescence (IF) or "chased" for various lengths of time by switching back to normal growth medium without Bac before staining with a polyclonal antibody against Bac. The drug is clearly taken up by HaCaT cells within 1 h and can persist within vesicular compartments for up to 24 h postentry (Fig. 3A). Additional experiments revealed that Bac failed to bind to the cell surface at 4°C but would readily enter cells within 15 min at 37°C, suggesting a fluid-phase entry pathway rather than receptor-mediated endocytosis (data not shown). To determine the nature of these Bac-containing vesicular structures, we performed a colocalization analysis using a panel of antibodies against different intracellular organelle markers. Bac was present in a variety of cellular compartments and most strongly colocalized with clathrin light chain, LAMP1, caveolin 1, syntaxin 6, and CD44. Moderate colocalization was observed with EEA1, Rab7, and flotillin 2, and low levels of Bac were colocalized with ER and Golgi markers calnexin and giantin (Fig. 3B).

Next, we assessed whether Bac colocalized with HPV16 during infection by IF and confocal microscopy. Cells were infected with HPV16 in the presence of Bac and fixed/processed for IF at different times postinfection. At 30 min, the virus (green signal) was present mainly on the cell surface while Bac (red signal) had already been endocytosed, although some punctate intracellular colocalization was observed (Fig. 3C). During the course of infection, the levels of colocalization between virus and drug generally increased, and by 16 h, the majority of the viral signal overlapped large amounts of Bac that had accumulated during the infection (Fig. 3C). The fast internalization of Bac and its colocalization
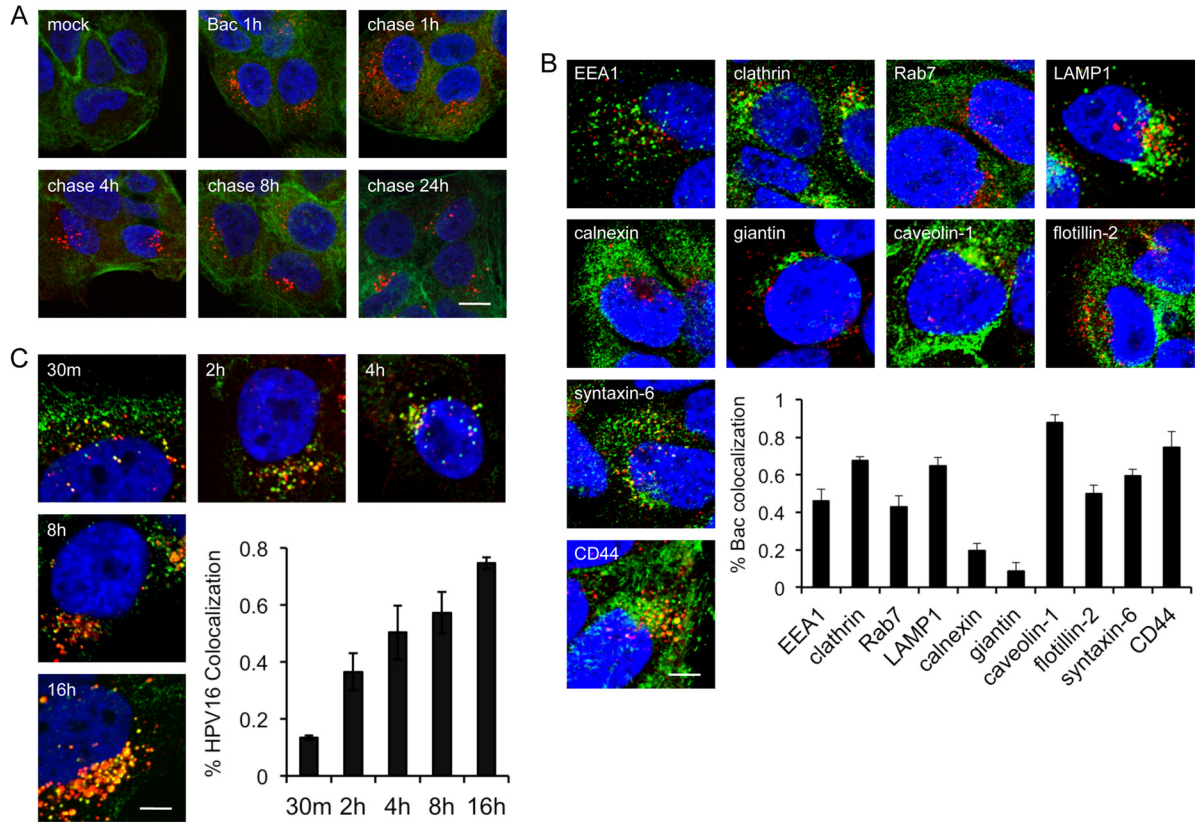
FIG 3 Cellular uptake of bacitracin. (A) Pulse-chase experiment. Cells were mock treated or pulsed with Bac for 1 h at 37°C before they were either fixed for IF or chased with normal medium for the indicated times before fixation and IF. Actin was stained with AF488-phalloidin (green), Bac was detected with sheep anti-Bac polyclonal antibody and AF555 donkey anti-sheep antibody (red), and nuclei were stained with DAPI (blue). (B) Colocalization of internalized Bac with cellular markers. HaCaT cells were grown in 5 mM Bac for 8 h prior to fixation and IF and as described in Materials and Methods. Bac was stained with sheep anti-Bac polyclonal and AF555 donkey anti-sheep (red) antibodies. Cells were counterstained with antibodies against the indicated markers (green), as described in Materials and Methods. Nuclei were stained with DAPI (blue). The inset shows colocalization of Bac signal with the indicated cellular markers, quantified by the Manders method, as described in Materials and Methods. (C) Colocalization of Bac with HPV16. Cells were infected in medium plus Bac for the indicated times prior to fixation for IF. HPV16 L1 was stained with rabbit anti-L1 K75 polyclonal and AF488 donkey anti-rabbit (green) antibodies. Bac was stained with sheep anti-Bac polyclonal and AF555 donkey anti-sheep (red) antibodies. Nuclei were stained with DAPI (blue). Bars, 10 μm (A); 5 μm (B and C).

with HPV16 during infection help to explain some of the time-dependent inhibition data (Fig. 2F). Bac added at late stages postentry can likely "catch up" to the internalized virus and cause inhibition (Fig. 2F, solid line). Alternatively, Bac can likely "out-run" the virus in the withdrawal experiments, with the virions at the later stages (8 h) of infection being susceptible to Bac inhibition while the virions present upstream in the entry pathway, due to the continuous stream of viral uptake in the presence of Bac, may be able to continue with infection and account for ~50% infectivity after withdrawal of the drug at 8 h (Fig. 2F, dashed line).

Bacitracin does not affect HPV16 trafficking or exposure of hidden epitopes within L1 or L2. During viral entry, trafficking, and uncoating, a number of conformational changes occur that result in exposure of inaccessible epitopes in both the L1 and L2 capsid proteins. A C-terminal epitope of HPV16 L1, residues 427 to 445, is initially inaccessible but becomes available to bind monoclonal antibody H16.U4 (9, 10) as early as 4 h postinfection (16). Likewise, another region of L1, residues 303 to 313, is located in the central cavities underneath each of the L1 pentamers. This region is available for binding to the monoclonal antibody L1-7 (58) only after capsid disassembly/vDNA uncoating, around 8 h

postinfection (70). We tested the effects of Bac on exposure of these epitopes during infection by IF and found no differences from normal infection (Fig. 4A and B). The polyclonal antibody K75 (52) was used to visualize total L1 protein in these experiments. These results agree with previous observations by Western blotting that Bac had no effect on capsid disassembly/degradation (Fig. 2C and D). Consistent with this, Bac treatment had no effect on the lysosomal trafficking of HPV16 (Fig. 4C).

During the course of infection, an N-terminal region of L2, residues 17 to 36, becomes exposed on the virion surface. This portion of L2 is recognized by the monoclonal antibody RG-1, binding of which neutralizes infection (22). The activities of two cellular enzymes, the proprotein convertase furin (and other related proprotein convertase [PC] enzymes) and the peptidyl-prolyl isomerase CyPB, are necessary for exposure of the RG-1 epitope (4, 13). Biochemical inhibition of either furin or CyPB prevents exposure of the RG-1 epitope and causes a blockage of HPV16 infection at late stages postentry (4, 49). Bac has been reported to have pleiotropic effects, including the inhibition of certain proteases (3, 35, 46, 81), and it is conceivable that Bac could have some inhibitory effects on either furin or CyPB, thereby blocking infection at a late stage by
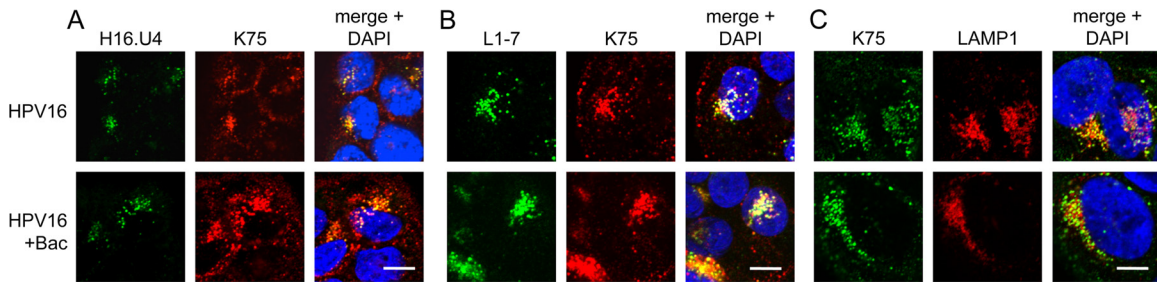
FIG 4 Bacitracin does not block endocytic trafficking or exposure of buried L1 epitopes. Cells were infected in medium with or without Bac for 4 h (A) or 8 h (B and C) prior to fixation and permeabilization for IF as described in Materials and Methods. (A) L1 was stained with mouse monoclonal H16.U4 and AF488 anti-mouse (green) with rabbit polyclonal K75 and AF555 anti-rabbit (red). (B) L1 was stained with mouse monoclonal L1-7 and AF488 anti-mouse (green) with rabbit polyclonal K75 and AF555 anti-rabbit (red). (C) L1 was stained with rabbit polyclonal K75 and AF488 anti-rabbit (green), and LAMP1 was stained with mouse anti-LAMP1 and AF555 anti-mouse (red). Nuclei of all samples were stained with DAPI (blue). Bars, 10 μm (A and B); 5 μm (C).

preventing exposure of the RG-1 epitope. We therefore tested the effects of Bac on RG-1 epitope exposure by immunostaining with the RG-1 antibody at 4 h postinfection. Bac treatment caused no changes in RG-1 exposure (Fig. 5), implying that Bac is not blocking HPV16 infection by interfering with either furin or CyPB.

Bacitracin prevents viral genome accumulation at nuclear PML bodies. Residence in the acidic endo-/lysosomal compartment is thought to trigger capsid disassembly and permit endosomal penetration of L2/vDNA complexes, which are then transported into the nucleus through an unknown mechanism where they accumulate at nuclear PML bodies at late times postinfection. To directly monitor the fate of the vDNA during infection, we used a DNA labeling system based on the incorporation of the thymidine analog 5-ethynyl-2′-deoxyuridine (EdU) during virus production in 293TT cells. EdU-labeled HPV16 was used to study the effects of Bac and the endosomal acidification inhibitor bafilomycin A (BafA) on vDNA accumulation at PML bodies at 42 h postinfection by IF and confocal microscopy. Disassembled L1 capsid protein was also monitored with the L1-7 monoclonal antibody in these experiments. Mock-infected cells had no detectable EdU or L1 signal, demonstrating that EdU detection has very low background (Fig. 6B and C). The majority of the vDNA in HPV16-infected cells displayed punctate nuclear fluorescence (Fig. 6G) and was colocalized with nuclear PML bodies (Fig. 6J, arrows). A smaller portion of vDNA was observed in cytoplasmic vesicles (Fig. 6G and I). L1 capsid was present in perinuclear cy-

toplasmic compartments, some of which colocalized with cytoplasmic vDNA signal, but was never observed in the nucleus (Fig. 6H and I).

Bac caused a very strong inhibition of vDNA accumulation at PML bodies, despite its enhancing effects on viral uptake (Fig. 6K to O). Occasionally, a very small amount of vDNA was seen colocalized with PML bodies (Fig. 6O, arrow), in agreement with the low but measurable levels of infectivity routinely observed with 5 mM Bac. The majority of the vDNA signal that was present in Bac-treated samples occurred in cytoplasmic vesicles, colocalizing with L1 signal (Fig. 6N). The bulk of the L1 signal in the Bac-treated samples likely represents degraded (25-kDa) L1, as this was the predominant form at 12 h and later times postinfection (Fig. 2D and data not shown). The small quantity of L1 that colocalized with vDNA may represent intact particles that are in an earlier stage of infection due to the enhancement effect of Bac, which causes a continuous stream of viral uptake (Fig. 2A to E).

BafA blocks endosomal acidification and is a potent inhibitor of HPV16 (14, 65). BafA treatment also blocked vDNA localization at PML bodies and caused large amounts of cytoplasmic vDNA signal, which colocalized strongly with L1 in vesicular structures (Fig. 6P to T). Surprisingly, uncoated L1-7 signal was detectable in the presence of BafA, implying that some capsid disassembly can occur in the absence of acid-dependent proteases and that a low level of proteolytic activity persists in the presence of BafA. Indeed, we observed by Western blotting of infected cells that treatment with BafA at concentrations that block HPV16 infection will impair L1 degradation but does not completely block it (see Fig. S5 in the supplemental material). The persistence of the vDNA signal and its complete colocalization with L1 in the BafA-treated cells suggest that during normal infection only a fraction of vDNA escapes the endosomal system and accumulates at PML bodies to initiate infection while the majority is degraded in lysosomes along with L1 capsid.

Unlike BafA, Bac treatment did not preserve the vDNA signal, implying that Bac does not inhibit lysosomal degradation of vDNA. This finding is consistent with our observations that Bac has no effect on L1 degradation (Fig. 2D) or capsid disassembly and localization to lysosomes (Fig. 4A and B and Fig. 5). Taken together, these data support the notion that Bac blocks infection by preventing endosomal penetration of uncoated vDNA.

Bacitracin does not block γ-secretase. Recent work has shown that host cell γ-secretase activity is required for HPV16 infection
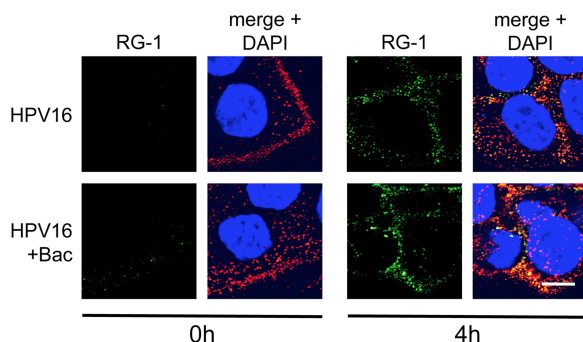

FIG 5 Bacitracin does not affect exposure of the L2 RG-1 epitope. Cells were infected in medium with or without Bac for 0 h or 4 h before fixation and permeabilization for IF as described in Materials and Methods. L2 was stained with mouse monoclonal RG-1 and AF488 anti-mouse (green) with rabbit polyclonal K75 and AF555 anti-rabbit (red). Bar, 10 μm.
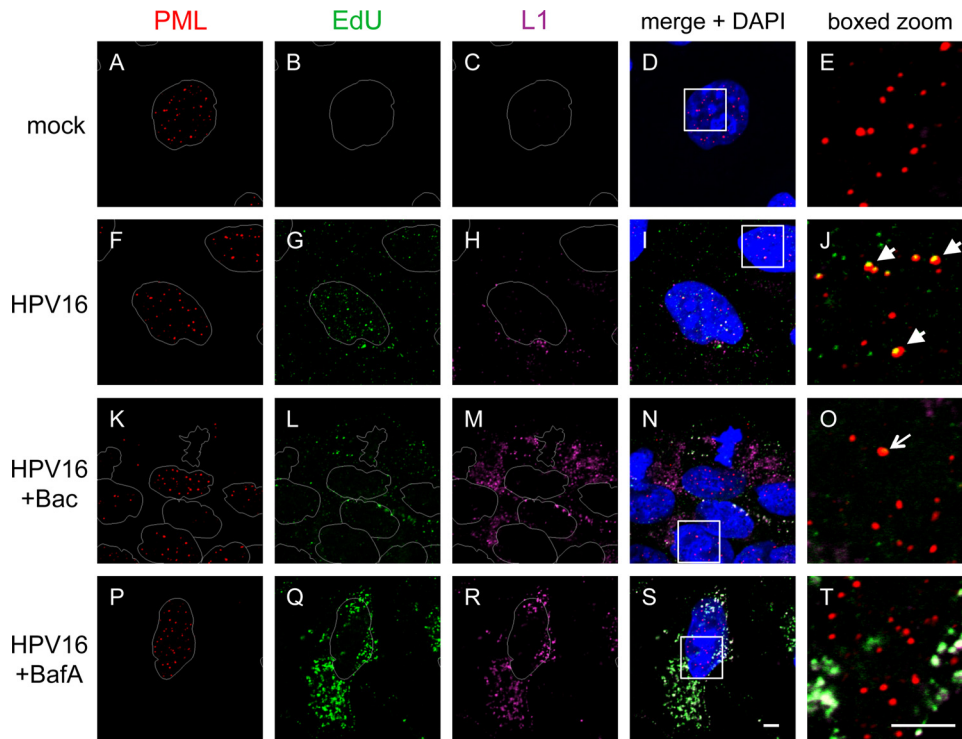
FIG 6 Bacitracin prevents vDNA localization at nuclear PML bodies. Cells were mock treated (A to E) or infected with HPV16 in medium alone (F to J) or in the presence of either Bac (K to O) or BafA (P to T) for 42 h prior to fixation and IF and as described in Materials and Methods. Nuclear PML bodies were stained with rabbit anti-PML and AF555 anti-rabbit (red). EdU-labeled vDNA was stained via click chemistry labeling with AF488-N$_3$ (green), as described in Materials and Methods. L1 was stained with the mouse monoclonal L1-7 and AF633 anti-mouse (purple pseudocolor). Nuclei were stained with DAPI. Bars, 5 μm.

and that inhibition of γ-secretase prevents HPV16 vDNA escape from the endosomal compartment, without interfering with uncoating or trafficking to lysosomes (28, 36). This inhibitory phenotype is identical to that of Bac, and the antiviral activity of Bac could be explained if it acts as a γ-secretase inhibitor. γ-Secretase is an integral membrane protease complex that acts on a wide variety of transmembrane (TM) substrate proteins by cleaving their TM domains. One of the better-characterized γ-secretase substrates is the amyloid precursor protein (APP). We utilized an APP-based reporter construct encoding a Myc-tagged C99 fragment of APP to determine if Bac abrogated γ-secretase activity. Cells were transfected with pAPP-C99-Myc reporter and treated with the γ-secretase inhibitors XXI and DAPT or Bac, and the Myc-tagged C99 fragment was detected by Western blotting. γ-Secretase cleavage across the TM domain of C99-Myc generates a smaller Myc-tagged fragment, the APP intracellular domain (AICD). In the absence of inhibitors, the AICD fragment can be seen as the upper band of a doublet (Fig. 7A, lane 2). The lower band (marked with an asterisk) is due to an aberrant proteolytic event, is not an indicator of γ-secretase activity, and has been reported by other groups using this pAPP-C99-Myc reporter (27). Inhibition of γ-secretase by XXI and DAPT prevented the generation of AICD (Fig. 7A, lanes 3 and 4), but Bac had no effect on AICD levels (Fig. 7A, lanes 5 and 6). Comparable results were observed using a similar reporter based on Notch, another γ-secretase substrate (79). These data show that Bac blocks HPV16 infection via a γ-secretase-independent mechanism.

A reducing agent can partially rescue HPV16 from bacitracin inhibition. Although Bac is not a specific inhibitor of PDIs, it has been reported to inhibit the reductive function of PDI by a number of different cell-based and *in vitro* assays (26, 35, 41, 66). We therefore hypothesized that the addition of the cell-permeant reductant β-mercaptoethanol (β-ME) might relieve the inhibition caused by Bac. Cells were infected in medium with or without Bac for 48 h. After an initial 8 h of continuous infection in medium with or without Bac, the viral inoculum was replaced with fresh medium with or without Bac containing an increasing amount of β-ME. Infection in the presence of the β-ME gradient with or without Bac continued for 12 h at 37°C, after which time the reducing medium was replaced with medium with or without Bac and infection continued for an additional 28 h. In the absence of β-ME, infection levels reached only 4% in the presence of Bac. Low concentrations of β-ME did not change the inhibitory effect of Bac, but higher levels of β-ME resulted in partial rescue of HPV16 infection (Fig. 7B). Bac inhibition was repressed nearly ~3-fold by transient treatment with 16 mM β-ME, suggesting that disulfide reduction and cellular redox may play an important role in endosomal penetration of vDNA during the late stages of HPV16 cell invasion.

PDI and ERp72 are important for HPV16 infection. As a preliminary search for cellular reductases involved in HPV16 infection, we screened a small panel of PDI family members by siRNA knockdown. Transient knockdown of PDI and ERp72 decreased infection by ~35% and ~65%, respectively (Fig. 8A). In contrast, knockdown of the PDI family member ERp57 consistently resulted in slightly higher levels of infectivity, al-
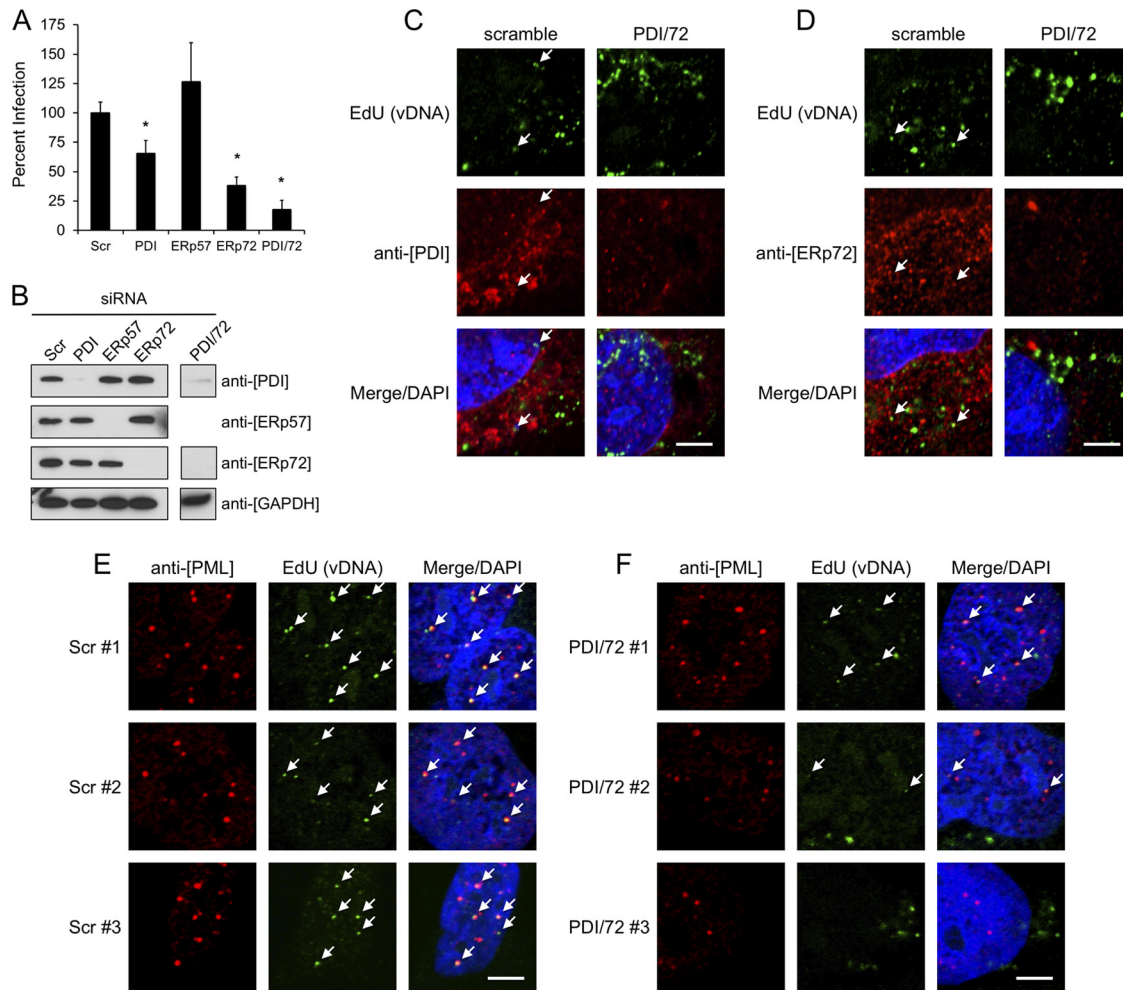
FIG 7 Bacitracin does not block γ-secretase but may inhibit a critical reductive function during infection. (A) Cellular γ-secretase activity assay. Cells were transfected with an irrelevant GFP plasmid (mock) or the γ-secretase reporter pAPP-C99-Myc expressing a Myc-tagged C99 fragment of the amyloid precursor protein for 6 h prior to replacement of growth medium with or without the indicated drugs. Cell lysates were harvested at 24 h for SDS-PAGE and Western blotting assays with the indicated antibodies. Cleavage of the C99 fragment by γ-secretase generates the smaller AICD fragment, marked with an arrow. The asterisk denotes a nonspecific cleavage product of C99, which has been reported by others in the literature using this same plasmid (27). (B) Transient reduction can partially repress Bac inhibition. Cells were infected with virus with or without Bac for 8 h prior to removal of the virus and addition of fresh medium with or without Bac and supplemented with the indicated concentrations of β-ME. Cells were incubated with the reductant with or without Bac for 12 additional hours prior to switching back to medium with or without Bac without β-ME reductant and incubation for another 28 h (48-h total infection time) prior to measurement by luciferase assay. Infections were performed in triplicate, with error bars representing standard errors of the means.

though these increases were not statistically significant (Fig. 8A). Combined knockdown of both PDI and ERp72 blocked infection by ~80%. Strong and specific knockdown of the PDI family members was confirmed by Western blotting of the infected-cell lysates (Fig. 8B). Immunofluorescence of siRNA-transfected HaCaT cells infected with EdU-labeled virus was used to determine the effects of dual PDI-ERp72 knockdown on viral entry and vDNA-PML colocalization and to look for overlap of the PDI family members with vDNA during infection. No obvious defects in viral entry were observed for the combined knockdown compared to the scramble control (Fig. 8C and D). Little colocalization was observed between the PDI family members and vDNA; arrows indicate the minimal overlap for PDI (Fig. 8C) and ERp72 (Fig. 8D). The accumulation of vDNA at nuclear PML bodies was affected by dual PDI-ERp72 siRNA knockdown (Fig. 8E). The inhibitory effect was partial, but overall fewer viral genomes were observed at PML bodies and the EdU signal was generally weaker than that observed in

the scramble control (Fig. 8F). The incomplete blockage of vDNA-PML colocalization is not surprising since dual knockdown still displayed about ~20% infectivity (Fig. 8A).

DISCUSSION

We investigated the effects of the widely used PDI inhibitor Bac on HPV16 infection. Initial experiments demonstrated a clear dose-dependent inhibition of HPV16 and other HPV types. Studies on the mechanisms of Bac inhibition unexpectedly revealed a Bac-dependent enhancement of cell binding and continuous cellular uptake of HPV16 through an infectious pathway. Although further experiments will be necessary to reveal the mechanisms of this increased binding and uptake, the fact that it occurs during the 4°C binding step indicates that the phenomenon likely occurs through some nonenzymatic means. Bac has metal-chelating activity and will form 1:1 complexes with divalent metal ions, including Cu^{2+}, Ni^{2+}, Co^{2+}, Zn^{2+}, and Mn^{2+} (44), and possibly Mg^{2+} and Ca^{2+} as well (47). This metal-chelating activity, particularly that of Zn^{2+}, is critical for the antibiotic effects of Bac against Gram-positive bacteria (71). The structure and activity of many cell surface proteins and extracellular matrix components, including integrins and metalloproteases, can be greatly influenced by divalent metal ions (25, 73, 74). A possible mechanism of Bac-dependent enhancement of HPV16 binding might therefore involve the sequestration of certain divalent metal ions by the high concentrations of Bac present. Removal of key metals could change the conformation or alter the activity of certain cellular proteins, resulting in increased HPV16 binding and continuous viral entry. We are currently working to investigate this Bac-dependent enhancement phenomenon.

Bac blocked ~95% of infection despite the enhancement at early times. Further studies on the inhibitory mechanisms revealed a time dependency, with viral inhibition occurring at a late stage of cell invasion. Blockage of infection at late times postentry was inconsistent with the membrane-impermeant nature of Bac. This discrepancy was reconciled by our finding that Bac can readily enter cells through endocytosis, accumulating within various intracellular compartments and colocalizing with HPV16 at late times postinfection. We hypothesize that Bac causes viral inhibition by interfering with the activity of a cellular factor within these sites of colocalization at late times postinfection.

Bac caused enhanced viral entry and had no deleterious effect on HPV16 trafficking to lysosomes, capsid disassembly, or exposure of L1 and L2 epitopes. RG-1 epitope exposure is dependent on cellular furin and cyclophilin, suggesting that Bac does not block HPV16 infection by interfering with these cellular functions. Using viral particles encapsidating EdU-labeled vDNA, we observed blockage of endosomal penetration and failure of vDNA to accumulate within nuclear PML bodies. Bac prevents the endosomal penetration of vDNA, leading to destruction of viral genomes within the endo-/lysosomal compartment. Bafilomycin A, an inhibitor of endosomal acidification, also blocks nuclear/PML accumulation of vDNA, but genomes are not destroyed in this case. Rather, BafA causes accumulation of vDNA within the endo-/lysosomal compartment, suggesting that normally vDNA either escapes or is destroyed by acid-dependent lysosomal nucleases.

Although the inhibitory phenotype of Bac matches that of γ-secretase inhibitors (28, 36), Bac does not block cellular γ-secretase activity. Bac therefore blocks a cellular factor other

FIG 8 siRNA knockdown of PDI family members. (A) HaCaT cells were transfected with siRNAs against PDI family members or a scrambled control (Scr) for 24 h prior to infection with HPV16, as described in Materials and Methods. Luciferase activity was measured 24 h postinfection. Results are from three independent experiments, each performed in triplicate, with error bars representing standard errors of the means; *, $P < 0.001$, paired two-tailed Student's t test. (B) Confirmation of specific siRNA knockdown by Western blotting of siRNA-transfected/infected-cell lysates. (C and D) HaCaT cells plated on coverslips were transfected with siRNAs prior to continuous infection with EdU-labeled HPV16 for 16 h. Cells were stained with rabbit anti-PDI in panel C and rabbit anti-ERp72 in panel D, both with AF555 anti-rabbit (red). EdU-labeled vDNA was stained with AF488-N₃ (green) as described above. (E and F) Localization of vDNA (green) and PML bodies (red) in Scr (E) or combined PDI/ERp72 (F) siRNA-transfected cells. Three representative images are shown for each condition. Arrows indicate colocalized signals; bars, 5 μm.

than γ-secretase that is also critical for endosomal penetration of viral genome. The inhibitory effects of Bac were partially negated by transient treatment of infected cells with the membrane-permeant reductant β-ME. This suggests that Bac may be inhibiting the reducing activity of a PDI-like enzyme that is normally involved in HPV16 infection. We screened the abundantly expressed PDI family members PDI, ERp57, and ERp72 by siRNA knockdown and identified a potential role for ERp72 and, to a lesser extent, PDI in HPV16 infection. Dual knockdown of both PDI and ERp72 blocked infection by ~80% and reduced vDNA-PML colocalization, similar to the phenotype observed with Bac. Despite this inhibition, overlap between vDNA and PDI/ERp72 during infection was marginal. This could be due to the high concentration of these proteins in the ER with only trace amounts present in other compartments, or this may be suggestive of an indirect role for PDI and ERp72 in HPV infection. Although PDI family members are primarily

localized to the ER, where they catalyze disulfide redox reactions, the canonical KDEL-based ER retention system is not 100% efficient and PDI, ERp57, and ERp72 can be secreted, complexing with additional factors on the on the cell surface (75, 80). These enzymes could therefore be present in the endosomal compartment, with small amounts being taken up from the surface during endocytosis. PDI family members have independent, overlapping, and cooperative substrate specificity and can exist within multiprotein complexes composed of various PDIs, molecular chaperones, and ER stress proteins (24, 42, 59, 76, 82). It remains to be determined if PDI and ERp72 directly interact with HPV16 and are direct targets of Bac or whether PDI and ERp72 act in a redox network upstream of a cellular reductase to modulate HPV16 infection.

Potential viral targets of such a cellular disulfide reductase activity include both the L1 and L2 capsid proteins. The HPV16 capsid exists in an oxidized state, with adjacent L1 pentamers

cross-linked together by disulfide bonds (38, 45, 57). Laboratory-produced virions are artificially oxidized during the maturation step of production (7, 48). The organotypic epithelial tissue culture model (43), a more physiologically relevant system of HPV production, was shown to have a redox gradient similar to that of skin with the uppermost layers existing in an oxidized state (11). HPV virions produced in this system and wart-derived HPVs are therefore likely to be in an oxidized state as well. Polyomavirus capsids are similarly built from pentamers of the major capsid protein VP1, and neighboring pentamers are disulfide bonded. SV40 and related polyomaviruses enter cells through lipid raft-mediated endocytosis and retrograde traffic to the ER, where they utilize PDI family members and components of the cellular ER-assisted degradation (ERAD) machinery to uncoat and translocate their viral genomes into the cell cytosol for nuclear transport (18, 23, 39, 40, 61, 78). Our data suggest that, unlike polyomaviruses, HPV16 uncoating involves proteolytic degradation of L1 in the endosomal pathway rather than disulfide reduction and that Bac had no effect on L1 degradation or uncoating and exposure of buried epitopes.

With regard to L2 as a potential target for a Bac-sensitive cellular reductase, our previous work has shown that L2 is oxidized in mature virions, containing an intramolecular disulfide bond between Cys22 and Cys28 (8). The disulfide between these two highly conserved cysteines is positioned right in the center of the RG-1 epitope (residues 17 to 36), and the furin-dependent exposure of this region has been shown to be absolutely critical for infection and endosomal penetration of viral genome (13). Bac does not interfere with furin cleavage or exposure of the RG-1 epitope but could potentially block a PDI-like enzyme that may normally reduce the C22-C28 disulfide. Detection of L2 17-36 exposure by RG-1 antibody binding and immunofluorescence is independent of redox state, as the monoclonal RG-1 can bind equally well to both reduced and oxidized L2 (data not shown; see also reference 21), so RG-1 epitope exposure is therefore not an indicator of L2 redox status. Reduction of the C22-C28 disulfide during infection could act as a molecular switch, enabling L2 to adopt the proper conformation to facilitate transfer of the vDNA across the endosomal membrane.

This work reveals that Bac has an unusual time-dependent reciprocal effect on HPV16 infection, enhancing virus binding and entry but blocking endosomal penetration of L2/vDNA. The mechanisms through which Bac prevents the cytoplasmic translocation of vDNA are not yet known but may involve inhibition of a cellular reductase activity. siRNA knockdown experiments implicate PDI and ERp72 in HPV16 infection, but more work is needed to understand their precise roles. Given the crucial role of L2 in endosomal penetration of vDNA, the recently identified Cys22-Cys28 disulfide bond in L2 (8) represents a likely target for such a reductive function, and investigations toward this end are ongoing. Although Bac has been FDA approved since 1948 and is widely used as an over-the-counter antibacterial topical ointment, its use as an anti-HPV preventative is questionable due to its allergenic properties (31) and the millimolar concentrations required for inhibition. Bac may prove to be a valuable tool in identifying important cellular factors involved in the molecular events of HPV16 infection, and this study justifies additional investigation into the contribution of PDI family members and the L2 disulfide bond in HPV16 infection.

REFERENCES

1. **Abramoff MD, Magelhaes PJ, Ram SJ.** 2004. Image processing with ImageJ. Biophotonics Int. **11**:36–42.
2. **Abromaitis S, Stephens RS.** 2009. Attachment and entry of Chlamydia have distinct requirements for host protein disulfide isomerase. PLoS Pathog. **5**:e1000357.
3. **Bennett RG, Hamel FG, Duckworth WC.** 2003. An insulin-degrading enzyme inhibitor decreases amylin degradation, increases amylin-induced cytotoxicity, and increases amyloid formation in insulinoma cell cultures. Diabetes **52**:2315–2320.
4. **Bienkowska-Haba M, Patel HD, Sapp M.** 2009. Target cell cyclophilins facilitate human papillomavirus type 16 infection. PLoS Pathog. **5**:e1000524.
5. **Bolte S, Cordelieres FP.** 2006. A guided tour into subcellular colocalization analysis in light microscopy. J. Microsc. **224**:213–232.
6. **Buck CB, et al.** 2008. Arrangement of L2 within the papillomavirus capsid. J. Virol. **82**:5190–5197.
7. **Buck CB, Thompson CD, Pang YS, Lowy DR, Schiller JT.** 2005. Maturation of papillomavirus capsids. J. Virol. **79**:2839–2846.
8. **Campos SK, Ozbun MA.** 2009. Two highly conserved cysteine residues in HPV16 L2 form an intramolecular disulfide bond and are critical for infectivity in human keratinocytes. PLoS One **4**:e4463.
9. **Carter JJ, Wipf GC, Benki SF, Christensen ND, Galloway DA.** 2003. Identification of a human papillomavirus type 16-specific epitope on the C-terminal arm of the major capsid protein L1. J. Virol. **77**:11625–11632.
10. **Christensen ND, et al.** 1996. Surface conformational and linear epitopes on HPV-16 and HPV-18 L1 virus-like particles as defined by monoclonal antibodies. Virology **223**:174–184.
11. **Conway MJ, et al.** 2009. Tissue-spanning redox gradient-dependent assembly of native human papillomavirus type 16 virions. J. Virol. **83**:10515–10526.
12. **Day PM, Baker CC, Lowy DR, Schiller JT.** 2004. Establishment of papillomavirus infection is enhanced by promyelocytic leukemia protein (PML) expression. Proc. Natl. Acad. Sci. U. S. A. **101**:14252–14257.
13. **Day PM, Gambhira R, Roden RBS, Lowy DR, Schiller JT.** 2008. Mechanisms of human papillomavirus type 16 neutralization by L2 cross-neutralizing and L1 type-specific antibodies. J. Virol. **82**:4638–4646.
14. **Day PM, Lowy DR, Schiller JT.** 2003. Papillomaviruses infect cells via a clathrin-dependent pathway. Virology **307**:1–11.
15. **Day PM, Schiller JT.** 2009. The role of furin in papillomavirus infection. Future Microbiol. **4**:1255–1262.
16. **Day PM, et al.** 2007. Neutralization of human papillomavirus with monoclonal antibodies reveals different mechanisms of inhibition. J. Virol. **81**:8784–8792.
17. **Ellgaard L, Ruddock LW.** 2005. The human protein disulphide isomerase family: substrate interactions and functional properties. EMBO Rep. **6**:28–32.
18. **Engel S, et al.** 2011. Role of endosomes in simian virus 40 entry and infection. J. Virol. **85**:4198–4211.
19. **Florin L, et al.** 2006. Identification of a dynein interacting domain in the papillomavirus minor capsid protein L2. J. Virol. **80**:6691–6696.
20. **Florin L, et al.** 2004. Nuclear translocation of papillomavirus minor capsid protein L2 requires Hsc70. J. Virol. **78**:5546–5553.
21. **Gambhira R, Jagu S, Karanam B, Day PM, Roden R.** 2009. Role of L2 cysteines in papillomavirus infection and neutralization. Virol. J. **6**:176.

22. **Gambhira R, et al.** 2007. A protective and broadly cross-neutralizing epitope of human papillomavirus L2. J. Virol. **81:**13927–13931.

23. **Gilbert J, Ou W, Silver J, Benjamin T.** 2006. Downregulation of protein disulfide isomerase inhibits infection by the mouse polyoma virus. J. Virol. **80:**10868–10870.

24. **Grubb S, Guo L, Fisher EA, Brodsky JL.** 2012. Protein disulfide isomerases contribute differentially to the endoplasmic reticulum-associated degradation of apolipoprotein B and other substrates. Mol. Biol. Cell **23:** 520–532.

25. **Hadler-Olsen E, Fadnes B, Sylte I, Uhlin-Hansen L, Winberg JO.** 2011. Regulation of matrix metalloproteinase activity in health and disease. FEBS J. **278:**28–45.

26. **Hassan MH, et al.** 2011. Potentiation of the reductase activity of protein disulphide isomerase (PDI) by 19-nortestosterone, bacitracin, fluoxetine, and ammonium sulphate. J. Enzyme Inhib. Med. Chem. **26:**681–687.

27. **Heilig EA, Xia W, Shen J, Kelleher RJ III.** 2010. A presenilin-1 mutation identified in familial Alzheimer disease with cotton wool plaques causes a nearly complete loss of gamma-secretase activity. J. Biol. Chem. **285:** 22350–22359.

28. **Huang HS, Buck CB, Lambert PF.** 2010. Inhibition of gamma secretase blocks HPV infection. Virology **407:**391–396.

29. **Ishii Y, et al.** 2007. Thiol-reactive reagents inhibits intracellular trafficking of human papillomavirus type 16 pseudovirions by binding to cysteine residues of major capsid protein L1. Virol. J. **4:**110.

30. **Ishii Y, Tanaka K, Kanda T.** 2003. Mutational analysis of human papillomavirus type 16 major capsid protein L1: the cysteines affecting the intermolecular bonding and structure of L1-capsids. Virology **308:**128–136.

31. **Jacob SE, James WD.** 2004. From road rash to top allergen in a flash: bacitracin. Dermatol. Surg. **30:**521–524.

32. **Jiang XM, Fitzgerald M, Grant CM, Hogg PJ.** 1999. Redox control of exofacial protein thiols/disulfides by protein disulfide isomerase. J. Biol. Chem. **274:**2416–2423.

33. **Johnson KM, et al.** 2009. Role of heparan sulfate in attachment to and infection of the murine female genital tract by human papillomavirus. J. Virol. **83:**2067–2074.

34. **Kämper N, et al.** 2006. A membrane-destabilizing peptide in capsid protein L2 is required for egress of papillomavirus genomes from endosomes. J. Virol. **80:**759–768.

35. **Karala AR, Ruddock LW.** 2010. Bacitracin is not a specific inhibitor of protein disulfide isomerase. FEBS J. **277:**2454–2462.

36. **Karanam B, et al.** 2010. Papillomavirus infection requires gamma secretase. J. Virol. **84:**10661–10670.

37. **Kines RC, Thompson CD, Lowy DR, Schiller JT, Day PM.** 2009. The initial steps leading to papillomavirus infection occur on the basement membrane prior to cell surface binding. Proc. Natl. Acad. Sci. U. S. A. **106:**20458–20463.

38. **Li M, Beard P, Estes PA, Lyon MK, Garcea RL.** 1998. Intercapsomeric disulfide bonds in papillomavirus assembly and disassembly. J. Virol. **72:** 2160–2167.

39. **Lilley BN, Gilbert JM, Ploegh HL, Benjamin TL.** 2006. Murine polyomavirus requires the endoplasmic reticulum protein Derlin-2 to initiate infection. J. Virol. **80:**8739–8744.

40. **Magnuson B, et al.** 2005. ERp29 triggers a conformational change in polyomavirus to stimulate membrane binding. Mol. Cell **20:**289–300.

41. **Mandel R, Ryser HJ, Ghani F, Wu M, Peak D.** 1993. Inhibition of a reductive function of the plasma membrane by bacitracin and antibodies against protein disulfide-isomerase. Proc. Natl. Acad. Sci. U. S. A. **90:** 4112–4116.

42. **Meunier L, Usherwood Y-K, Chung KT, Hendershot LM.** 2002. A subset of chaperones and folding enzymes form multiprotein complexes in endoplasmic reticulum to bind nascent proteins. Mol. Biol. Cell **13:**4456–4469.

43. **Meyers C, Frattini MG, Hudson JB, Laimins LA.** 1992. Biosynthesis of human papillomavirus from a continuous cell line upon epithelial differentiation. Science **257:**971–973.

44. **Ming LJ, Epperson JD.** 2002. Metal binding and structure-activity relationship of the metalloantibiotic peptide bacitracin. J. Inorg. Biochem. **91:**46–58.

45. **Modis Y, Trus BL, Harrison SC.** 2002. Atomic model of the papillomavirus capsid. EMBO J. **21:**4754–4762.

46. **Pascual I, et al.** 2011. Effect of divalent cations on the porcine kidney cortex membrane-bound form of dipeptidyl peptidase IV. Int. J. Biochem. Cell Biol. **43:**363–371.

47. **Podlesek Z, Comino A.** 1994. Antagonists of bacitracin. Lett. Appl. Microbiol. **19:**102–104.

48. **Pyeon D, Lambert PF, Ahlquist P.** 2005. Production of infectious human papillomavirus independently of viral replication and epithelial cell differentiation. Proc. Natl. Acad. Sci. U. S. A. **102:**9311–9316.

49. **Richards RM, Lowy DR, Schiller JT, Day PM.** 2006. Cleavage of the papillomavirus minor capsid protein, L2, at a furin consensus site is necessary for infection. Proc. Natl. Acad. Sci. U. S. A. **103:**1522–1527.

50. **Roberts JN, et al.** 2007. Genital transmission of HPV in a mouse model is potentiated by nonoxynol-9 and inhibited by carrageenan. Nat. Med. **13:** 857–861.

51. **Rogelj S, Reiter KJ, Kesner L, Li M, Essex D.** 2000. Enzyme destruction by a protease contaminant in bacitracin. Biochem. Biophys. Res. Commun. **273:**829–832.

52. **Rommel O, et al.** 2005. Heparan sulfate proteoglycans interact exclusively with conformationally intact HPV L1 assemblies: basis for a virus-like particle ELISA. J. Med. Virol. **75:**114–121.

53. **Ryser HJ, Levy EM, Mandel R, DiSciullo GJ.** 1994. Inhibition of human immunodeficiency virus infection by agents that interfere with thiol-disulfide interchange upon virus-receptor interaction. Proc. Natl. Acad. Sci. U. S. A. **91:**4559–4563.

54. **Salic A, Mitchison TJ.** 2008. A chemical method for fast and sensitive detection of DNA synthesis in vivo. Proc. Natl. Acad. Sci. U. S. A. **105:** 2415–2420.

55. **Sapp M, Bienkowska-Haba M.** 2009. Viral entry mechanisms: human papillomavirus and a long journey from extracellular matrix to the nucleus. FEBS J. **276:**7206–7216.

56. **Sapp M, Day PM.** 2009. Structure, attachment and entry of polyoma- and papillomaviruses. Virology **384:**400–409.

57. **Sapp M, Fligge C, Petzak I, Harris JR, Streeck RE.** 1998. Papillomavirus assembly requires trimerization of the major capsid protein by disulfides between two highly conserved cysteines. J. Virol. **72:**6186–6189.

58. **Sapp M, et al.** 1994. Analysis of type-restricted and cross-reactive epitopes on virus-like particles of human papillomavirus type 33 and in infected tissues using monoclonal antibodies to the major capsid protein. J. Gen. Virol. **75:**3375–3383.

59. **Satoh M, Shimada A, Kashiwai A, Saga S, Hosokawa M.** 2005. Differential cooperative enzymatic activities of protein disulfide isomerase family in protein folding. Cell Stress Chaperones **10:**211–220.

60. **Schelhaas M.** 2010. Come in and take your coat off—how host cells provide endocytosis for virus entry. Cell. Microbiol. **12:**1378–1388.

61. **Schelhaas M, et al.** 2007. Simian virus 40 depends on ER protein folding and quality control factors for entry into host cells. Cell **131:**516–529.

62. **Schiller JT, Day PM, Kines RC.** 2010. Current understanding of the mechanism of HPV infection. Gynecol. Oncol. **118:**S12–S17.

63. **Schneider MA, Spoden GA, Florin L, Lambert C.** 2011. Identification of the dynein light chains required for human papillomavirus infection. Cell. Microbiol. **13:**32–46.

64. **Selinka HC, et al.** 2007. Inhibition of transfer to secondary receptors by heparan sulfate-binding drug or antibody induces noninfectious uptake of human papillomavirus. J. Virol. **81:**10970–10980.

65. **Selinka HC, Giroglou T, Sapp M.** 2002. Analysis of the infectious entry pathway of human papillomavirus type 33 pseudovirions. Virology **299:**279–287.

66. **Smith AM, et al.** 2004. A high-throughput turbidometric assay for screening inhibitors of protein disulfide isomerase activity. J. Biomol. Screen. **9:**614–620.

67. **Smith JL, Campos SK, Ozbun MA.** 2007. Human papillomavirus type 31 uses a caveolin 1- and dynamin 2-mediated entry pathway for infection of human keratinocytes. J. Virol. **81:**9922–9931.

68. **Smith JL, Campos SK, Wandinger-Ness A, Ozbun MA.** 2008. Caveolin-1-dependent infectious entry of human papillomavirus type 31 in human keratinocytes proceeds to the endosomal pathway for pH-dependent uncoating. J. Virol. **82:**9505–9512.

69. **Smith JL, Lidke DS, Ozbun MA.** 2008. Virus activated filopodia promote human papillomavirus type 31 uptake from the extracellular matrix. Virology **381:**16–21.

70. **Spoden G, et al.** 2008. Clathrin- and caveolin-independent entry of human papillomavirus type 16—involvement of tetraspanin-enriched microdomains (TEMs). PLoS One **3:**e3313.

71. **Stone KJ, Strominger JL.** 1971. Mechanism of action of bacitracin: complexation with metal ion and C55-isoprenyl pyrophosphate. Proc. Natl. Acad. Sci. U. S. A. **68:**3223–3227.

72. **Surviladze Z, Dziduszko A, Ozbun MA.** Essential roles for soluble virion-

associated heparan sulfonated proteoglycans and growth factors in human papillomavirus infections. PLoS Pathog. **8:**e1002519.

73. **Takagi J, Petre BM, Walz T, Springer TA.** 2002. Global conformational rearrangements in integrin extracellular domains in outside-in and inside-out signaling. Cell **110:**599–611.

74. **Takagi J, Springer TA.** 2002. Integrin activation and structural rearrangement. Immunol. Rev. **186:**141–163.

75. **Turano C, Coppari S, Altieri F, Ferraro A.** 2002. Proteins of the PDI family: unpredicted non-ER locations and functions. J. Cell. Physiol. **193:** 154–163.

76. **Vandenbroeck K, Martens E, Alloza I.** 2006. Multi-chaperone complexes regulate the folding of interferon-gamma in the endoplasmic reticulum. Cytokine **33:**264–273.

77. **Walboomers JM, et al.** 1999. Human papillomavirus ia a necessary cause of invasive cervical cancer worldwide. J. Pathol. **189:**12–19.

78. **Walczak CP, Tsai B.** 2011. A PDI family network acts distinctly and coordinately with ERp29 to facilitate polyomavirus infection. J. Virol. **85:** 2386–2396.

79. **Weyand NJ, Calton CM, Higashi DL, Kanack KJ, So M.** 2010. Presenilin/gamma-secretase cleaves CD46 in response to Neisseria infection. J. Immunol. **184:**694–701.

80. **Willems SH, et al.** 2010. Thiol isomerases negatively regulate the cellular shedding activity of ADAM17. Biochem. J. **428:**439–450.

81. **Zaya NE, Vaughan EE, Shah SK, Castignetti D.** 2002. Bacitracin: substantiation and elimination of contaminating proteolytic activity and use of an affinity chromatography ligand to purify a siderophore-degrading enzyme. Curr. Microbiol. **44:**71–74.

82. **Zhang Y, Baig E, Williams DB.** 2006. Functions of ERp57 in the folding and assembly of major histocompatibility complex class I molecules. J. Biol. Chem. **281:**14622–14631.